

Transmission by presynaptic spike-like depolarization in the squid giant synapse

(chemical transmission/Ca current/depolarization–release coupling)

R. LLINÁS, M. SUGIMORI, AND S. M. SIMON

Department of Physiology and Biophysics, New York University Medical Center, 550 First Avenue, New York, New York 10016

Communicated by Eric R. Kandel, December 28, 1981

ABSTRACT Synaptic transmission produced by artificially generated presynaptic depolarizations, having the same waveform as normal presynaptic action potentials, was studied in the squid giant synapse. These simulated spikes produced synaptic transmission virtually indistinguishable from that obtained with the original presynaptic spike activation. The technique allows a direct determination of the onset and amplitude of the Ca current, I_{Ca} , triggered by the presynaptic action potential and the relationship between I_{Ca} and postsynaptic response. The results closely resemble theoretical predictions by a previously published model for synaptic transmission in this synapse and demonstrate that I_{Ca} occurs at the falling phase of the presynaptic spike.

A theoretical model for synaptic transmission has been developed from experimental data obtained by voltage clamping the presynaptic terminal of the distal giant synapse (1–3) in the squid stellate ganglion (4). To assess directly the validity of the model and to test further the relationship between presynaptic Ca entry and transmitter release, we designed voltage clamp experiments in which the command pulse simulated presynaptic action potentials. The technique used was similar to that introduced to determine the ionic conductances during action potentials (5). The action potential from a presynaptic terminal was recorded intracellularly and stored digitally. After pharmacological blockage of the sodium and potassium voltage-dependent conductances, g_{Na} and g_K , respectively, the recorded action potential was reintroduced at the presynaptic terminal through the voltage clamp circuit. Because synaptic transmission obtained under such conditions mimicked closely that obtained prior to g_{Na} and g_K blockage, the present results indicate that such pharmacological treatment does not in itself alter the depolarization–release coupling mechanism. In addition, the technique allowed a direct determination of the onset, time course, and magnitude of the Ca current, I_{Ca} , generated by presynaptic action potentials. These results closely resemble those predicted by the above-mentioned theoretical model. Because the present techniques allow direct control of the time and voltage parameters of the presynaptic depolarization, they are deemed useful in studying chemical synaptic transmission. In particular, transmission changes after specific modifications in the waveform and amplitude of the presynaptic spike (6–8) or modifications of the ionic and pharmacological character of the external milieu may be investigated independently of the possible action of such variables on g_{Na} and g_K . In addition, the modulator effect of synaptic release also may be addressed directly (9, 10).

The publication costs of this article were defrayed in part by page charge payment. This article must therefore be hereby marked "advertisement" in accordance with 18 U. S. C. §1734 solely to indicate this fact.

MATERIALS AND METHODS

Experiments with *Loligo pealei* were carried out in Woods Hole, Massachusetts, at the Marine Biological Laboratory. The squid were chosen to have a mantle length of ≈ 10 cm, but smaller animals were also utilized. After decapitation, the stellate ganglia were isolated from the mantle and placed in a recording chamber for fine dissection. The recording techniques and the voltage clamp procedure have been described in detail (2). Briefly, the experimental procedure consisted of recording pre- and postsynaptic action potentials at the giant synapse prior to blockage of g_{Na} and g_K (see Fig. 1A). Two or three electrodes were introduced into the presynaptic terminal and one in the postsynaptic fiber at the junction site. The recordings obtained from these electrodes were digitized and stored on a Kennedy digital tape recorder. In addition, the presynaptic action potential was stored in a digital memory buffer having a resolution of 2 μ sec per point time and 25 μ V per point amplitude, which obviates most of the problems of reconstructing action potentials with voltage clamp techniques (11). Next, g_{Na} was blocked by addition of tetrodotoxin ($1 < \mu$ g/cc) (12) to the artificial seawater, and g_K was blocked by intracellular injection of tetraethylammonium ion (13) and external administration of 3- or 4-aminopyridine (5 mM) (14–17)*. In order to assess the viability of the preparation, I_{Ca} and the resulting postsynaptic potentials were determined with step voltage clamp pulses (2). The presynaptic action potentials stored in the digital buffer were then fed into the command amplifier of the voltage clamp circuit. In this manner, a voltage transient similar to the shape and amplitude of the recorded action potential was generated across the presynaptic membrane (Fig. 1B and C); however, the amplitude and duration of this simulated spike could be electronically controlled (see Fig. 2D–G). In synapses not damaged by impalement, this action-potential-like depolarization reproduced precisely the rate of rise and latency for the postsynaptic responses obtained prior to g_{Na} and g_K blockage (Fig. 1C).

Once a set of recordings was obtained, the Ca conductance, g_{Ca} , was blocked by addition of either 500 μ M CdCl₂ or 20 mM MnCl₂ to the bath. At these concentrations, these ions completely block Ca entry and synaptic transmission (3, 18) but do not change the passive properties of the membrane (Fig. 1E and F).

Ca currents were then obtained by subtracting the total current recorded after Ca blockage from the total current recorded prior to this blockage (Fig. 1F). This difference gives the onset,

Abbreviation: EPSP, excitatory postsynaptic potential.

* In a small proportion of experiments, 3- or 4-aminopyridine increased the synaptic delay by as much as 300 μ sec without affecting the onset of the presynaptic Ca current.

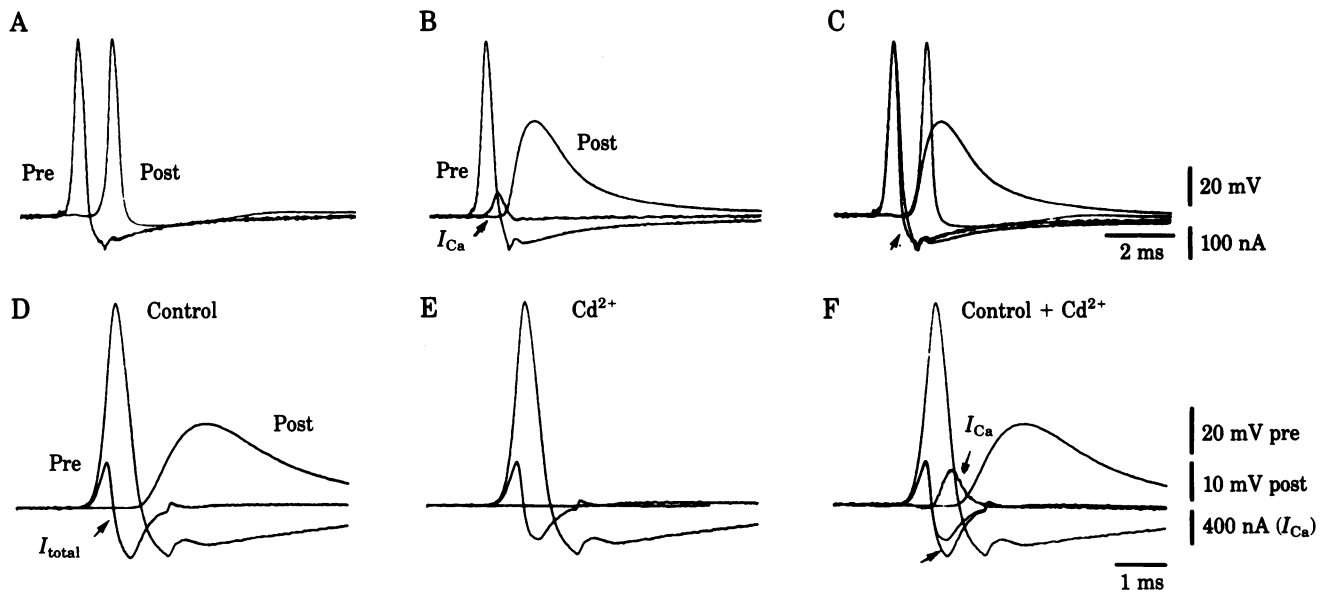


FIG. 1. Methodology utilized for the determination of I_{Ca} after a presynaptic action potential. (A) Simultaneous recordings of the presynaptic (Pre) and the postsynaptic (Post) action potentials prior to blockage of g_{Na} and g_K . (B) Use of the presynaptic action potential in A as a command voltage, generating a postsynaptic potential (Post). The I_{Ca} current triggering the release of transmitter is also shown. (C) Superposition of A and B, showing the similarity between original and simulated presynaptic action potentials and the similarity between delay and rate of rise of the postsynaptic responses. Arrow, the original action potential. (D–F) Techniques for determining I_{Ca} : from another synapse, the simulated presynaptic spike (Pre), total current (reduced leakage and I_{Ca}), and postsynaptic response (D); a similar experiment after addition of 0.5 mM $CdCl_2$ to the bath, showing the disappearance of the postsynaptic response (E); superposition of D and E, showing the difference (lower arrow) in inward current between D and E (F). Upper arrow, time course and amplitude of I_{Ca} . Note that the current calibration relates to I_{Ca} only.

magnitude, and time course of the I_{Ca} for a given presynaptic spike. In order to increase the resolution of our digital recordings, total current (Fig. 1 D and E) was stored after a reduction of the linear leakage-current component with a bridge circuit, the fraction of this reduction being proportional to the amplitude of the leakage current. This methodology affected neither the amplitude nor the time course of I_{Ca} because the identical leakage component was subtracted before and after g_{Ca} blockage. The same measurements of I_{Ca} were obtained by subtracting the total current generated by adding sequentially 10 spike-like depolarizations of 1/10th the amplitude of the original signal.

A similar measurement of I_{Ca} also can be obtained by subtracting the currents produced by artificial depolarizing action potentials from their hyperpolarizing counterparts. However, because of nonlinear passive membrane properties, on occasions there are slight phase shifts in the total-current record in response to voltage steps of different polarity that generate artifacts at the initial portion of the subtracted currents.

The current was measured either with reference to the return current electrode or with a third intracellular presynaptic microelectrode (2) as in Adrian's technique (19). This electrode also was used to test the degree of space clamping. Under normal conditions, the difference between these two potentials was less than 3%. However, because these two current-measuring systems generate very similar results after complete blockage of g_K , most experiments were performed with the two-electrode technique, which produces less injury to the presynaptic terminal. It is worth mentioning that the close agreement between these two current-measuring techniques supports previous results indicating that I_{Ca} is mostly restricted to the presynaptic terminal under study (1–3).

RESULTS

Reconstruction of Presynaptic Action Potentials and Determination of I_{Ca} . The wave shape of the action potential obtained

through the voltage clamp circuit was basically indiscernible from that originally recorded. This is seen in Fig. 1A, where the pre- and postsynaptic action potentials recorded prior to g_{Na} and g_K blockage are shown. The artificial presynaptic action potential recorded through the voltage clamp circuit after g_{Na} and g_K blockage is shown in Fig. 1B. A comparison of Fig. 1A and B (Fig. 1C) shows that the action potential-like voltage transient (Fig. 1B) is very similar to the original presynaptic spike (Fig. 1A). This artificial spike produces a synaptic potential (labeled post in Fig. 1B) having the same initial rate of rise and latency (Fig. 1C) as the original postsynaptic response. The I_{Ca} generated by the artificial spike is shown as an up-going transient in Fig. 1B.

The method for determining I_{Ca} is illustrated in Fig. 1 D–F, which shows the artificial spike and the total current (I_{total}). After addition of $CdCl_2$ to the external bath, there is a reduction of the latter part of I_{total} (only the reduced leakage current remains), and the postsynaptic potential is abolished (Fig. 1E). Superposition of the previous two current records (Fig. 1F) shows the difference between the total current (which includes I_{Ca}) and the leakage current. The computed difference is shown at twice the gain in Fig. 1F.

Relationship Between Amplitude of Presynaptic Spike-Like Depolarization and I_{Ca} . The latency and time course for I_{Ca} evoked by an artificial action potential is shown in detail in Fig. 2A for the same synapse illustrated in Fig. 1 D–F. Typically, this current has a late onset (at the falling phase of the action potential), a fast rate of rise, and a slightly slower rate of fall. This waveform is quite close to that predicted on the basis of the above-mentioned model for transmission. However, while the latency and amplitude of I_{Ca} matched extremely well, the falling time was slightly faster than predicted, as was the time constant of the tail current for this particular set of results. Indeed, the mean time constant of the tail current after a step voltage clamp pulse was found to be $331 \mu\text{sec} \pm 14 \text{ SD}$ from an n of 56 rather than that reported previously of $540 \mu\text{sec} \pm$

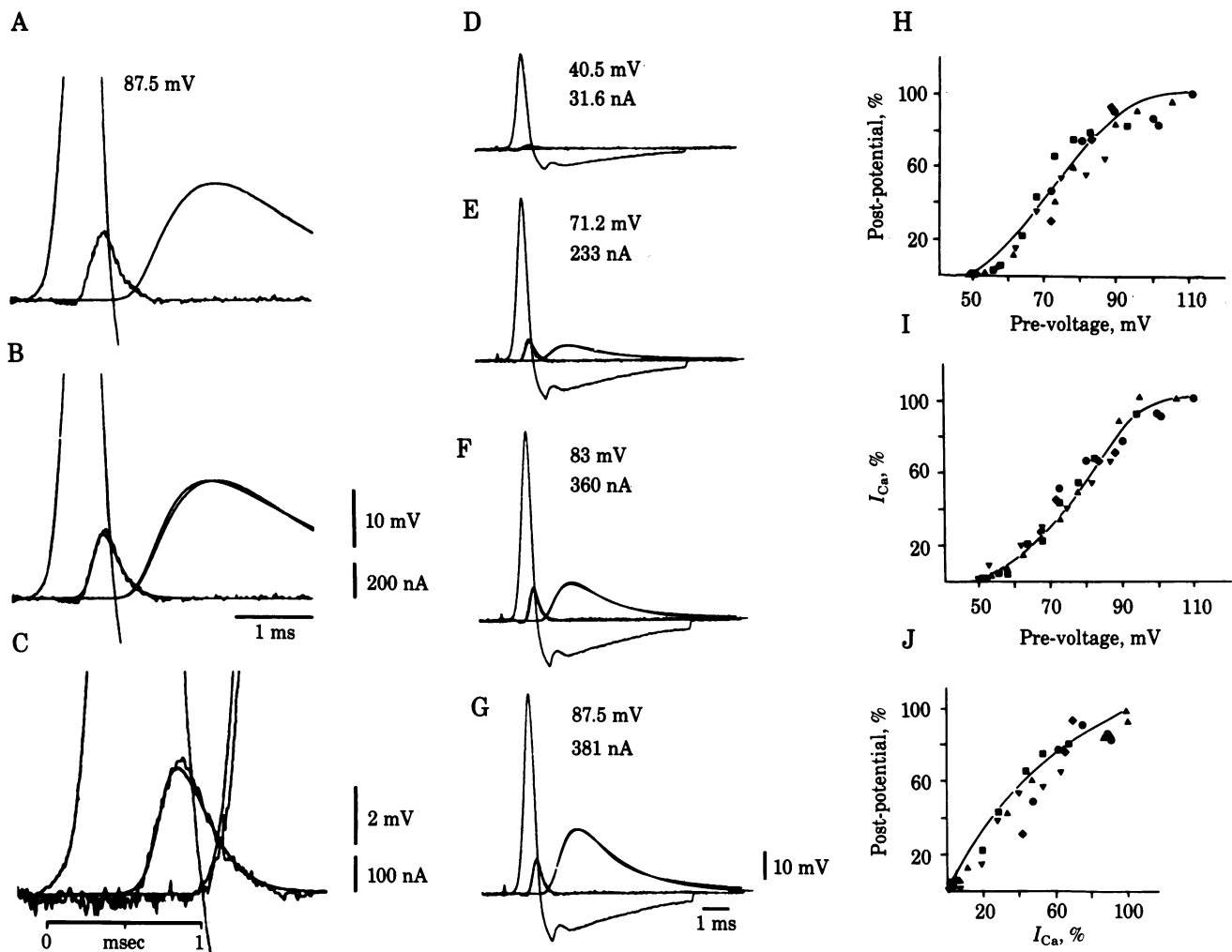


FIG. 2. Relationship between amplitude of simulated presynaptic spike, I_{Ca} , and postsynaptic potential. (A–C) Time course and amplitude of I_{Ca} evoked by a 87.5-mV artificial presynaptic spike (same as that in G). (A) Experimental results showing the truncated (due to high gain) presynaptic potential, the Ca current (noisy trace), and the postsynaptic response. (B) Results generated by the theoretical model, with the presynaptic spike in A superimposed on experimental results. (C) Same records as B at increased gain to demonstrate synaptic delay (onset of the presynaptic spike measured by linear extrapolation of rising phase to baseline). (D–G) Relationship of presynaptic-spike height to I_{Ca} and postpotential. The experimental and modeling results are superimposed as in B and C. The relationship between presynaptic voltage (pre-voltage) and post-synaptic potential (post-potential) (H), presynaptic voltage and I_{Ca} (I), and I_{Ca} and postsynaptic potential (J) are shown for five experiments. Because the absolute values of these variables differ with the size of the terminal, the results were normalized to give a clearer view of variability between preparations. The results from the theoretical model are shown as a continuous line in these three plots.

83 SD from an n of 68. This change reflects an increase in voltage clamp speed brought about by faster electronic circuit components. Because the time course for the fall of I_{Ca} (observable in Fig. 2A) and for the tail current was quite reproducible in our new results, we deemed it important to modify the voltage dependence of the forward and backward rate constants, k_1 and k_2 , in our model (2) to achieve a better fit with this new data. The change allowed a modification of the time constant for the theoretical tail I_{Ca} to match our experimental results. According to the model (2), each Ca channel is composed of n number of subunits, each of which exists in either of two states, S and S' . The transition between these states is governed by the rate constants, k_1 and k_2 . Thus,



A gate or channel, G , is open when all n subunits are in the S' state. \bar{S}' is the probability of a subunit being in the S' state, and the number of "open" channels, $[G]$, is proportional to $(\bar{S}')^n$, so $[G] = \text{total number of channels} \cdot (\bar{S}')^n$. Ca current is given by

$[G]$ times the current flow per gate, j . Thus,

$$I_{Ca} = [G] \cdot j.$$

The relevant points here are the forward and backward rate constants, k_1 and k_2 , and their dependence on membrane potential, V . The expressions for k_1 and k_2 are

$$\begin{aligned} k_1 &= k_1^0 \exp(\epsilon z_1 V / kT) \\ k_2 &= k_2^0 \exp(\epsilon z_2 V / kT). \end{aligned} \quad [1]$$

k_1^0 and k_2^0 are independent of membrane potential. ϵ is the elementary electric charge; k is Boltzman's constant; T is the temperature; and z_1 and z_2 designate the number of charges that move across the membrane by the transformation of S and S' into the activated transition state. These values reflect the dipole moment changes (normal to the membrane) between the open and transition state, z_1 , and the closed and transition state, z_2 . (For a full explanation of the model, see ref. 2.) The present modifications consisted in shifting the orientation of these dipoles so that in the closed state they sense 6% less and in the

open state 6% more of the electric energy field than previously. This brought the modeled I_{Ca} (Fig. 2 B and C) quite close to the currents obtained in most experiments without altering substantially the onset or amplitude of the "on" I_{Ca} in the model. [Modification of the value of n (cf. ref. 2) failed to achieve the small correction in the tail current time constant.]

Because the height and duration of the artificial action potentials could be varied, the relationship between these variables and the presynaptic current (and postsynaptic response) could be directly determined. Usually the amplitude of the simulated spike was varied from 40 to 110 mV as in Fig. 2 D–G, where I_{Ca} and the postsynaptic response elicited by a 1-msec artificial spike are shown at four amplitudes covering the steepest portion of the depolarization–release curve (40–90 mV). The I_{Ca} peak amplitudes in nanoamperes are given on each trace; for an 80-mV spike, I_{Ca} had a value of $309 \text{ nA} \pm 77 \text{ SD}$ for 13 experiments. These differences in I_{Ca} amplitude between synapses relate closely to the size of the presynaptic terminal under study. In Fig. 2 D–G, each of the records represents a superposition of the experimental and model results (as in Fig. 2 B and C). Note that the amplitude, time course, and duration of I_{Ca} for each record is close to that of the model for various amplitude action potentials, once the peak I_{Ca} was normalized for that resulting from an action potential of 75 mV. This was also the case for all synapses that have been superimposed on the model. A similar agreement may be seen for the postsynaptic potentials following the parameters of the original model (3). The relationship between the amplitude of the artificial action potential and the Ca current for five experiments is plotted in Fig. 2I, showing a typical S-shape that approaches a plateau near 110 mV from a 70-mV holding potential (absolute voltage, +40 mV), the minimum action potential required to generate a Ca current (Fig. 2I) or a synaptic potential (Fig. 2H) being, for this synapse, 45 mV from the holding potential (absolute potential, –25 mV). The S-shaped relationship is also very similar to that predicted by the model (solid lines). (To facilitate comparison, the current amplitude was normalized at 75-mV depolarization and expressed as a percentage of the highest value). As for the precise latency of the modeled excitatory postsynaptic potential (EPSP), a best fit was obtained where the minimum latency observed for the "off" EPSP ($\approx 200 \mu\text{sec}$) was added as a constant to the model as previously described (3).

Relationship Between Ca Current and Transmitter Release. Results obtained in these experiments indicate a first- to second-order relationship between Ca current and postsynaptic response (3, 15). The relationship between the amplitude of I_{Ca} and EPSP height is plotted for five synapses in Fig. 2J. This relationship also holds for total Ca charge and EPSP amplitude and has an average slope of 1.47, with a range of 1.01–2.08 for $n = 13$.

Another significant aspect of this research relates to the latency of transmitter release. The latency and amplitude for the postsynaptic response after tetrodotoxin (TTX) was exactly the same as that obtained prior to pharmacological manipulations. This is significant because even when the initial Ca^{2+} concentration was increased to 100 mM (in the absence of an initial Mg^{2+} concentration), addition of tetrodotoxin did not increase synaptic delay, indicating that I_{Ca} through the sodium channels (20) does not contribute to transmitter release. The latency between the onset of Ca entry and transmitter release is $375 \mu\text{sec} \pm 65 \text{ SD}$ for $n = 5$. This latency is, as expected from our model (ref. 2, i.e., first-order kinetics for the Ca fusion-promoting factor activation), slightly larger than that of the experimentally observed $200 \mu\text{sec}$ for the "off" potential generated by the tail I_{Ca} (2), which has a more abrupt onset and a larger amplitude. This slightly longer delay is also present in the results from the

model (with the above-mentioned proviso of a 200- μsec added delay) (Fig. 2C). These results indicate that, at least for single-spike transmission, an artificial action potential is as effective in releasing transmitter as is the original action potential itself. Some variability among synapses was seen in the latency of the postsynaptic response as measured from the onset of the presynaptic spike (on the order of 100–300 μsec). However, these latter differences were also present prior to the voltage clamp measurements.

The amplitude of the experimentally recorded postsynaptic response also varied among preparations. This reflects not only differences in the amount of transmitter released by a given terminal but also relates to the passive properties of the postsynaptic element, whose form changes drastically from one synapse to the next. The maximum postsynaptic response for a clamped presynaptic spike of 90 mV had a mean amplitude of $39.9 \text{ mV} \pm 3.8 \text{ SD}$ for $n = 13$.

DISCUSSION

The present findings indicate that after g_{Na} and g_K blockage, synaptic transmission has the same properties as observed prior to pharmacological intervention. This does not necessarily mean that g_{Na} and g_K have no presynaptic role other than to activate the voltage-dependent Ca conductance. Possibly they are quite significant in facilitating or depressing release if multiple action potentials are generated and in serving to regulate the active ionic transport and enzymatic activity required for protracted functioning (21).

The present set of results has determined experimentally the Ca currents generated by an action potential in the presynaptic terminal of a chemical synapse. The results indicate that the S-shaped curve relating presynaptic voltage to postsynaptic response (1, 6, 22) reflects largely the voltage-dependent properties of the Ca conductance (1, 3). Further, as concluded from modeling based on previous experimental results, the action potential releases transmitter through a Ca current that begins during the falling phase of the action potential—i.e., it is largely a tail current (1, 3). Indeed, this current is larger than the "on" current generated during a square pulse of the same amplitude and is slightly smaller than the tail I_{Ca} generated by the repolarization after a square pulse; I_{Ca} is not a trivial function of the waveform and amplitude of the action potential. The advantages of a tail Ca current in synaptic transmission are clear. First, if the increase in g_{Ca} comes late during the action potential, the onset of this current will be well matched to the increased driving force for Ca as the membrane potential returns to resting level. Thus, at the peak of the conductance, the driving force for Ca will be maximal. Because I_{Ca} is both voltage and time dependent, the amount of transmitter released will be related not only to the amplitude of the action potential but also to its duration. The larger the amplitude (up to 110 mV) and duration (up to the asymptote of the I_{Ca} "on" kinetics) and the faster the rate of fall of the action potential, the larger the amount of I_{Ca} . In short, because the amplitude of the tail current depends on the magnitude and duration of the transmembrane electric field, especially in the ranges present for the amplitude and duration of normal action potentials, modulation of these parameters will regulate *de facto* the amount of transmitter released.

This research was supported by Grants NS13742 and NS14014 from the National Institute of Neurological and Communicative Disorders and Stroke.

1. Llinás, R., Steinberg, I. Z. & Walton, K. (1976) *Proc. Natl. Acad. Sci. USA* 73, 2918–2922.

2. Llinas, R., Steinberg, I. Z. & Walton, K. (1981) *Biophys. J.* **33**, 289–321.
3. Llinas, R., Steinberg, I. Z. & Walton, K. (1981) *Biophys. J.* **33**, 323–351.
4. Young, J. Z. (1939) *Philos. Trans. R. Soc. London Ser. B* **229**, 465–503.
5. Starzak, M. E. & Starzak, R. J. (1978) *IEEE Trans. Biomed. Eng.* **25**, 201–204.
6. Miledi, R. & Slater, C. R. (1966) *J. Physiol. (London)* **184**, 473–498.
7. Shapiro, E., Castellucci, V. F. & Kandel, E. R. (1980) *Proc. Natl. Acad. Sci. USA* **77**, 629–633.
8. Takeuchi, A. & Takeuchi, N. (1962) *J. Gen. Physiol.* **45**, 1181–1193.
9. Dunlap, K. & Fishbach, G. D. (1978) *Nature (London)* **276**, 837–839.
10. Kupfermann, I. (1979) *Annu. Rev. Neurosci.* **2**, 447–465.
11. Cole, K. S. (1980) *Biophys. J.* **31**, 433–434.
12. Narahashi, T., Moore, J. W. & Scott, W. R. (1964) *J. Gen. Physiol.* **47**, 965–974.
13. Armstrong, C. M. & Binstock, L. (1965) *J. Gen. Physiol.* **48**, 859–872.
14. Llinas, R., Walton, K. & Bohr, V. (1976) *Biophys. J.* **16**, 83–86.
15. Meves, H. & Pichon, Y. (1977) *J. Physiol. (London)* **268**, 511–532.
16. Pelhate, M. & Pichon, Y. (1974) *J. Physiol. (London)* **242**, 90–91P.
17. Yeh, J. Z., Oxford, G. S., Wu, C. H. & Narahashi, T. (1976) *J. Gen. Physiol.* **68**, 519–535.
18. Kostyuk, P. G. & Krishtal, O. A. (1977) *J. Physiol. (London)* **270**, 545–568.
19. Adrian, R. H., Chandler, W. K. & Hodgkin, A. L. (1970) *J. Physiol. (London)* **208**, 607–644.
20. Baker, P. F., Hodgkin, A. L. & Ridgway, E. B. (1971) *J. Physiol. (London)* **218**, 709–755.
21. Rahamimoff, R., Lev-Tov, A. & Meiri, H. (1980) *J. Exp. Biol.* **89**, 5–18.
22. Katz, B. & Miledi, R. (1967) *J. Physiol. (London)* **192**, 407–436.